

The Interaction of Na(I), Ca(II), and Mg(II) Metal Ions with Duplex DNA: A Theoretical Modeling Study

DARRIN M. YORK

*Department of Chemistry, University of North Carolina, Chapel Hill, North Carolina 27514,
and Laboratory of Molecular Toxicology, National Institute of Environmental Health Sciences,
Research Triangle Park, North Carolina 27709*

TOM DARDEN

*Laboratory of Molecular Toxicology, National Institute of Environmental Health Sciences,
Research Triangle Park, North Carolina 27709*

DAVID DEERFIELD II

Pittsburgh Supercomputing Center, 4400 Fifth Avenue, Pittsburgh, Pennsylvania 15213

LEE G. PEDERSEN

*Department of Chemistry, University of North Carolina, Chapel Hill, North Carolina 27514,
and Laboratory of Molecular Toxicology, National Institute of Environmental Health Sciences,
Research Triangle Park, North Carolina 27709*

Abstract

DNA is a negatively charged biopolymer composed of monomeric nucleotides each carrying on average a net (-1) charge concentrated in the region of the phosphate backbone. In solution, the net negative charge of the molecule is presumably balanced by positively charged cations that interact with the DNA. Important questions arise as to the molecular details of the interaction of different cations with DNA. In this paper, we investigate the interaction of monovalent sodium ions and divalent magnesium and calcium ions with duplex DNA using molecular dynamics. Three 50 ps molecular dynamics simulations of the DNA sequence $d[CGCGAATTCGCG]_2$ have been performed in different ionic environments. Each system is constructed to be electrically neutral and is composed of the DNA duplex immersed in a large water bath containing a specific ionic species [Na(I), Mg(II), or Ca(II)]. The structural differences of the DNA itself as a result of interacting with each ionic species have been previously examined (D. M. York, T. Darden, D. Deerfield, II, and L. Pedersen, *J. Biomol. Struct. Dyn.*, submitted). In the current work, the ion-DNA and ion-water interactions are examined. The coordination shells of the ions and distributions around the phosphate anions are reported, and both show close encouraging agreement with available experimental work. The results of our studies indicate that the hydration state of the ion plays an important role in the direct coordination of the phosphate anions. Na(I) and Ca(II) ions prefer to coordinate the phosphate anions directly, whereas Mg(II) ions have a greater tendency to interact with phosphate anions as fully hydrated cations. © 1992 John Wiley & Sons, Inc.

1. Introduction

It has long been recognized from thermal denaturation experiments that metal ions have a stabilizing effect on DNA in solution. Furthermore, the degree of sta-

bilization has been shown to depend strongly on the nature of the metal ion [1,2]. In addition to having a stabilizing effect on charged polyanions such as DNA, metal ions have been known to be specifically involved in many biological processes such as inducing and stabilizing condensed forms of DNA [3], regulating transitions between various polynucleotide forms [4], and mediating the binding of metalloproteins to DNA [5]. Furthermore, metal ions have been used extensively as tools in molecular biology and as therapeutic drugs [6]. Hence, the nature of specific metal ion–DNA interactions is of current theoretical and experimental interest.

Theoretical descriptions of metal ion–DNA interactions have been developed based on solutions of the cylindrical Poisson–Boltzmann equation (PB) [7] and on the counterion condensation hypothesis (CC) proposed by Manning [8]. The Poisson–Boltzmann treatment models the DNA as a rigid, charged cylinder from which the radial density of ions can be obtained based on electrostatic considerations (for a review of this technique and its application to the electrolyte environment around DNA, see Pack et al. [9,10]). Alternatively, the counterion condensation treatment models the DNA as a linear charge density and involves consideration of two types of ionic species. Ions can be mobile but restricted to a small distance from the surface of the polyelectrolyte and, hence, “territorially-bound,” or else unrestricted and only weakly interacting with the DNA. The theory predicts a condensation of ions on the surface of the polyelectrolyte having a characteristic linear charge density. Both PB and CC treatments estimate the concentration of ions at the surface of the DNA to be on the order of 1 *M*. NMR studies of ions around DNA have shown these theories to be generally successful in predicting the properties of the mobile ions [11–13]. PB and CC treatments, however, do not address the behavior of highly specific “site-bound” ions, which may play an important role in determining the structural properties of DNA. An alternative approach to examining the behavior of site-bound ions to polyelectrolytes is via large-scale computer simulations. Several theoretical investigations of DNA–ion interactions have been made using molecular dynamics (MD) [14–17] and Monte Carlo (MC) [18,19] techniques.

In this presentation, we use MD simulations to investigate the interactions of three kinds of biologically significant metal ions [Na(I), Ca(II), and Mg(II)] that are believed to interact predominantly with the negatively charged phosphate backbone of the DNA [20]. Three simulations of the DNA sequence $d[\text{CGCGAATTCGCG}]_2$ in aqueous solution were performed, each in the presence of one type of ion placed around the phosphate anions so as to neutralize the charge of the DNA. The results of the specific ion–water and ion–phosphate interactions for the various ions have been characterized and compared with existing experimental work.

2. Methods

A. Systems

The crystal structure of the dodecamer sequence $d[\text{CGCGAATTCGCG}]_2$ [21] provided the initial coordinates for the heavy atoms (C, N, O, P), and Watson–Crick H-bonding hydrogens from which the positions of the protons were determined

and added accordingly to produce the unrefined starting geometry. Ions were added to the system to neutralize the net (-22) charge of the DNA molecule. In the first system, 22 monovalent sodium ions were coordinated* with each phosphate residue of the DNA (the 5' and 3' ends were not phosphorylated). In the systems containing either calcium or magnesium, the divalent metal ions were coordinated with alternating phosphate anions, beginning with the first nucleotide monomer and ending with the twenty-third (using the numbering scheme employed by Dickerson and co-workers [21]). Hence, for the divalent ion simulations, six ions were associated with strand 1 (nucleotides 1–12) and five were associated with strand 2 (nucleotides 13–24). Once the ions were arranged around the DNA, the resulting structure was immersed in a rectangular box of MC water so that there was a layer at least 10 Å thick around the entire complex. Any water molecules placed in van der Waals contact with the DNA complex were removed. This resulted in a total of 3446 water molecules for the calcium and magnesium ion systems and 3661 water molecules for the sodium ion system.

B. Simulations

The molecular mechanics and dynamics calculations were performed using a vectorized and parallelized version of AMBER (3.1) [22] generously provided to us by C. Singh at Scripps. This version of AMBER is an outgrowth of efforts of the Kollman group at UCSF [23]. Full charges were used for all residues; thus, each phosphate group carried a net charge of (-1), the monovalent ions had a ($+1$) charge, and the divalent ions each had ($+2$) charges. Hence, all simulations were performed on electrically neutral systems. The all-atom force field [24] was used; the Na(I), Mg(II), and Ca(II) parameters employed were resident in the parameter set (see [27]; for applications to phosphate–metal ion complexes, see [28]). The TIP3P water model was used [29], and an 8.0 Å nonbonded cutoff was employed with a constant dielectric ($\epsilon = 1$). The simulations were performed at 300 K, constant pressure, with periodic boundary conditions and an integration time step of 0.0005 ps. The SHAKE algorithm was used to constrain proton movements. The positions of the water molecules were initially allowed to relax over 9 ps of MD while the atomic positions of the complexed DNA remained fixed. The position restraints were then removed, and the entire system was relaxed with energy minimization to give the starting structure for full MD simulation. Initially, full MD was performed for 10 ps to equilibrate the system. Subsequently, 40 ps of production MD was performed to produce the final trajectory used in this analysis.

3. Results

Several quantities can be calculated from the simulation trajectory to describe the ion environment around a polyelectrolyte. One useful quantity is the spatial correlation function, or radial distribution function (RDF), denoted by $g_{ab}(r)$ [30].

* The monovalent and divalent ions were placed at a distance of 5 Å along the vector bisecting the O—P—O bond angle, the unit that contains a classical negative charge of (-1).

The RDF is a dimensionless quantity that has the important property that $\rho_a g_{ab}(r) 4\pi r^2 dr$ represents the average number of particles of type "a" in a shell of thickness $r + dr$ around a particle of type "b," where ρ_a is the number density of species "a." The average number of "a" particles within a sphere of radius r around a "b" particle is obtained from the running coordination number, $n_{ab}(r)$, defined by

$$n_{ab}(r) = \rho_a \int_0^r g_{ab}(r') 4\pi r'^2 dr'. \quad (1)$$

For a completely homogeneous system of noninteracting particles, $g_{ab}(r)$ is unity for all r within the system and $n_{ab}(r)$ is just $(4/3)\pi r^3 \rho_a$. For real solutions where particles interact, $g_{ab}(r)$ will be a more complicated function having peaks that indicate ordered "coordination shells" or "solvation shells." If $g_{ab}(r)$ displays a strong first peak, and then goes to zero, $n_{ab}(r)$ is an integer and represents the number of nearest "a" neighbors to our particle "b" of interest and is used to define the "coordination number" (CN) of the first solvation shell. If $g_{ab}(r)$ does not go to zero after its first maximum, the solvation shells are not clearly defined; however, if $g_{ab}(r)$ is nearly zero in the region following the first maximum, the CN can approximately be taken to be $n_{ab}(r_m^1)$, where r_m^1 is the first minimum in $g_{ab}(r)$. Analogously, CNs for successive coordination spheres are defined as the integral of $\rho_a g_{ab}(r) 4\pi r^2 dr$ in the region between successive minima, i.e.:

$$\text{CN}^{(n)} = \rho_a \int_{r_m^{(n-1)}}^{r_m^{(n)}} g_{ab}(r') 4\pi r'^2 dr' = n_{ab}(r_m^{(n)}) - n_{ab}(r_m^{(n-1)}). \quad (2)$$

It should be emphasized that as the minima of $g_{ab}(r)$ become less and less pronounced (farther away from zero) these definitions become less useful as a rigorous structural measure. Typically, only the first and second solvation shells are discussed in terms $g_{ab}(r)$.

In addition to CNs, another useful parameter that can be obtained from the radial distribution function is the average distance of the particles in a particular solvation shell. Viewing $\rho_a g_{ab}(r) 4\pi r^2$ as a probability function, the average distance of a particle in the "nth" coordination shell is given by

$$\langle r^{(n)} \rangle = \int_{r_m^{(n-1)}}^{r_m^{(n)}} r' P(r') dr', \quad \text{where} \quad P(r') = g_{ab}(r') r'^2 / \int_{r_m^{(n-1)}}^{r_m^{(n)}} g_{ab}(r'') r''^2 dr''. \quad (3)$$

In some instances, particularly when the coordination spheres are not well resolved, the maxima of $g_{ab}(r)$ are used as a measure of distance instead of $\langle r^{(n)} \rangle$. In this case, the interpretation is not an average distance, but a most probable distance. For fairly well-resolved, symmetrical maxima, these two quantities are usually similar.

Another useful property for describing liquid structure is the lifetime τ_M , which is defined as the average time a particle spends in a particular coordination sphere

before exchanging with another particle outside the sphere. This quantity is sometimes discussed in terms of an exchange rate, which is related to the lifetime by $k_{exc} = 1/\tau_M$.

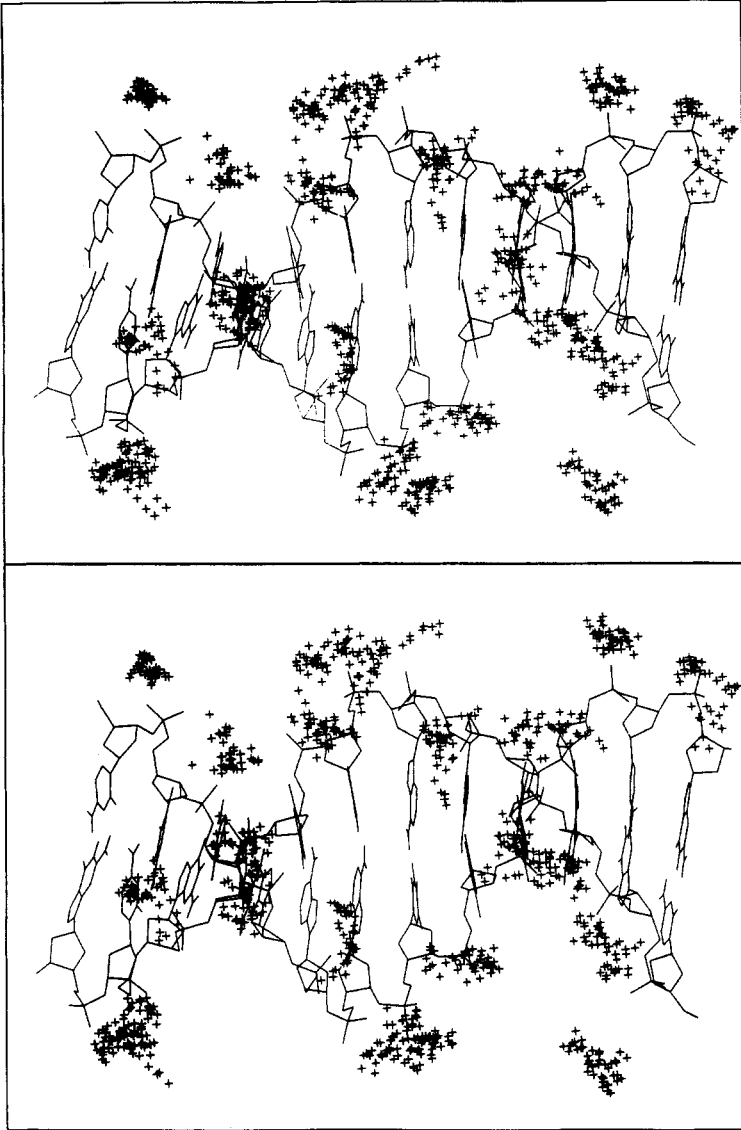
In this study, the hydration structure of metal ions in aqueous solution around DNA are examined. Only three negatively charged moieties were observed to interact with the first two coordination spheres of the ions: (1) water oxygens, (2) phosphinyl oxygens, and (3) phosphoester oxygens (O3', O5'). We restrict the discussion of solvation around the ions to these species. The structural environment of the ions are described by the radial distribution function of oxygens around a particular ion [Na(I), Ca(II), or Mg(II)]. The radial distribution function for each ion–oxygen pair was obtained by sampling a total of 1200 time intervals over 40 ps of MD. Figure 1 shows a stereopicture of the average sodium ion structure with the ion distribution indicated by hatch marks.

A. Metal Ion–Water Interactions

Figure 2 shows $g_{ab}(r)$ and $n_{ab}(r)$ for water oxygens (OW) around Na(I), Ca(II), and Mg(II) metal ions, and Table I compares the resulting average CNs and distances from the simulations to experimental values [29–33]. Table II gives the metal ion–water oxygen lifetimes for the first and second coordination spheres and compares them to values reported in the literature [34].

The magnesium RDF shows a very sharp peak centered around 2.0 Å. The average coordination distance of 2.03 Å is slightly less than the value 2.12 Å determined by X-ray diffraction [32]. The first hydration shell is well defined, as indicated by $g_{ab}(r)$ going to zero in the region 2.3–3.4 Å and the corresponding horizontal slope of the running integration number. The average CN for water oxygens is 5.6 (Table I), whereas if the contributions from the phosphinyl oxygens are included, the value is exactly 6.0, the same value observed from X-ray diffraction experiments. No exchange of water oxygens was observed for Mg(II) during the course of the simulation (hence, the RDFs go identically to zero after the first maximum). This is expected since the lifetime of a water oxygen in the first coordination sphere of magnesium is on the order of 2.0×10^6 ps. The region between 3.5 and 5.0 shows a relatively well-ordered second hydration shell centered around 4.3 Å and having a mean water oxygen CN of 11.8. This is less than the value of 15 reported from MD studies of MgCl₂ in aqueous solution [32] because the ions are not completely surrounded by a continuum of water due to the nearby DNA molecule. Exchange of water in the second coordination sphere of Mg(II) was observed with an estimated lifetime of 0.9 ps.

The Ca(II)–water oxygen RDF shows a first solvation peak around 2.5 Å with significantly reduced amplitude relative to that of Mg(II). The running CN also has a corresponding slight (+) slope in the region 3.0–4.0 Å separating the first and second solvation shells, indicating a less definite boundary. Nonetheless, the first and second hydration shells are fairly well resolved and reasonably narrow. The mean first coordination distance is 2.49 Å, in good agreement with experimental results from neutron scattering [31] (2.46 Å) and X-ray diffraction [30] (2.39 Å). The first CN of water oxygens for the larger Ca(II) ion is 6.7, and when contributions from the other oxygens are included, it is 7.6. Experimentally, the first CN for



Na (I)

Figure 1. Stereopicture of DNA with the Na(I) ion distribution displayed as hatch marks. The displayed DNA structure is an average structure from 10 to 50 ps of the simulation.

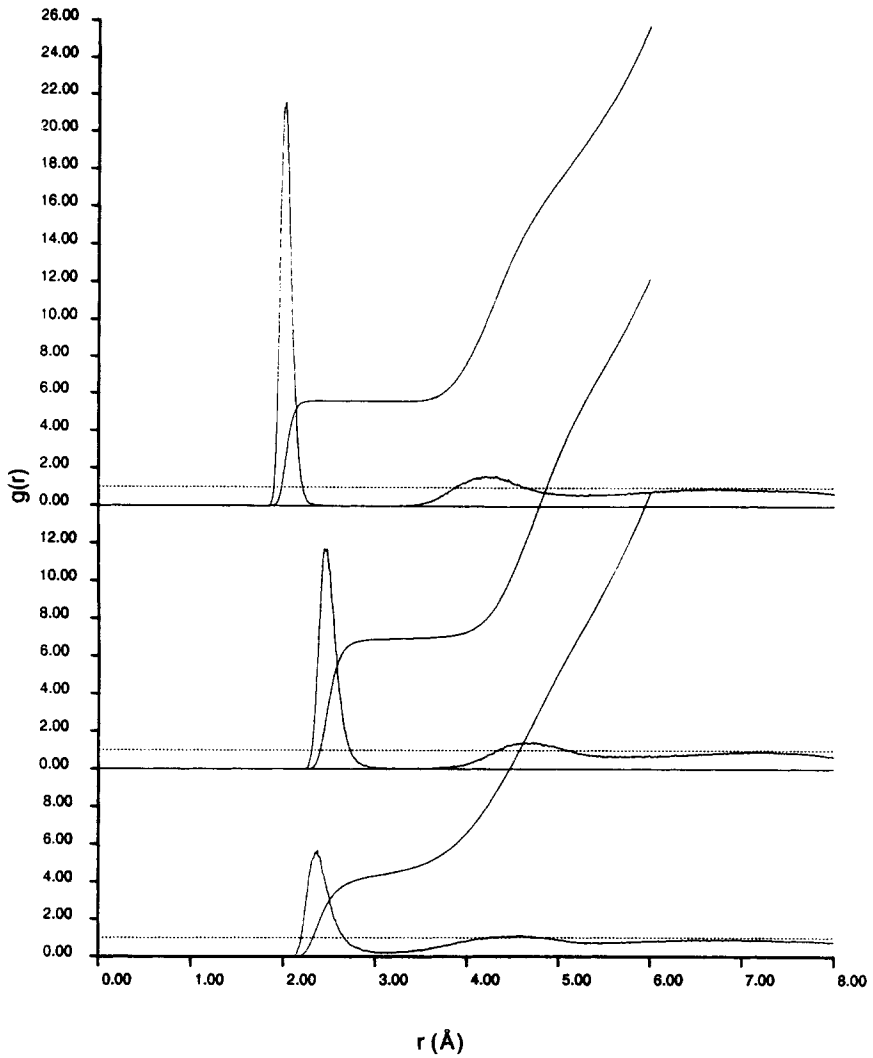
Na(I),Ca(II),Mg(II)--OW

Figure 2. RDF and running CN for ions surrounded by water oxygens.

TABLE I. Average coordination numbers (CN) and solvation distances ($\langle r \rangle$) of water oxygens surrounding the various ions.

| Ion | MD | | | | | EXP | | Ref. |
|---------|---------------------------|---------------------------|-----|------|------|---------------------------|---------|------|
| | $\langle r_1 \rangle$ (Å) | $\langle r_2 \rangle$ (Å) | CN1 | CN1* | CN2 | $\langle r_1 \rangle$ (Å) | CN1 | |
| Na (I) | 2.42 ± 0.10 | 4.62 ± 0.34 | 4.0 | 5.0 | 12.0 | 2.42 | 4.0 (X) | [29] |
| | | | | | | 2.20 | (Q) | [33] |
| Ca (II) | 2.49 ± 0.08 | 4.72 ± 0.28 | 6.7 | 7.6 | 12.7 | 2.39 | 6.9 (X) | [30] |
| | | | | | | 2.46 | 10 (N) | [31] |
| | | | | | | 2.40 | (Q) | [33] |
| Mg (II) | 2.03 ± 0.05 | 4.34 ± 0.29 | 5.6 | 6.0 | 11.8 | 2.12 | 6.0 (X) | [32] |
| | | | | | | 1.95 | (Q) | [33] |

Comparisons of values obtained from the simulations (MD) are made with experimental studies (EXP) of X-ray diffraction (X), neutron scattering (N), and ab initio calculations of monohydrated ions (Q). The calculated coordination number for any oxygen (water, phosphinyl, or phosphoester) in the first solvation sphere of each ion has also been included (CN1*).

aqueous calcium ions has not been well established, and measurements from different experiments show a wide range of values. Additionally, the coordination values are sensitive to concentration. The values reported in the literature for 1 M calcium from neutron scattering and X-ray diffraction are 10.0 and 6.9, respectively. The concentration of divalent ions in the simulations is 0.2 M. Waters in the first hydration sphere of Ca(II) are observed to exchange, having average lifetimes of 2 ps, agreeing with the experimentally measured value (Table II). The second hydration sphere (4.0–5.5 Å) is centered around 4.7 Å and contains roughly 12.7 waters, significantly less than the value of 24 observed in MD simulations of an aqueous CaCl₂ solution [30]. Again, the reason for this is that (1) other oxygen moieties populate the hydration sphere and (2) the nearby DNA molecule excludes water from surrounding the ions on all sides. Exchange in the second hydration shell of Ca(II) is comparable to that observed for Mg(II), with an estimated lifetime of 0.8 ps.

The RDF for Na(I) has a significantly less sharp first hydration peak centered around 2.4 Å. The average Na(I)–water oxygen distance is 2.42 Å with a corresponding CN of 4.0, in agreement with the experimental results [29], 2.42 Å and

TABLE II. Metal ion–water oxygen lifetimes (τ_M) estimated from the simulations and comparison with experimental values (EXP) [34].

| Ion | $\tau_M(1)$ | $\tau_M(2)$ | $\tau_M(1)$ EXP |
|---------|-------------|-------------|--------------------|
| Na (I) | 1–2 ps | 0.5 ps | 2 ps |
| Ca (II) | 2 ps | 0.8 ps | 2 ps |
| Mg (II) | > 40 ps | 0.9 ps | 2×10^6 ps |

4.0, respectively. The second solvation shell is seen as a broad symmetrical peak centered around 4.6 Å. The hydration spheres are not as well defined since in the region in between peaks (2.8–3.4 Å), $g_{ab}(r)$ does not go to zero. This is also evident by the increased positive slope of the running CN in this region. Hence, the exchange rate for water oxygens in the first and second solvation shells is faster, with average lifetimes of approximately 1.1 and 0.5 ps, respectively. These are within qualitative agreement with the expected lifetimes of alkali and alkaline earth metals, which are predicted to have a lower limit of 2 ps [34].

B. Metal Ion–Phosphinyl Oxygen Interactions

Figure 3 shows the RDF of phosphinyl oxygens for Na(I), Ca(II), and Mg(II) ions. Table III gives the corresponding average coordination distances and numbers and compares some of the results to ab initio calculations.

The RDF for Mg(II) shows a sharp peak around 1.9 Å corresponding to a well-defined first coordination sphere, with an average coordination distance of 1.86 Å, which is in agreement of the value of 1.89 Å obtained from ab initio studies of Mg(II) bound to dimethylphosphate [25]. The first CN for Mg(II) is 0.4. One should keep in mind that the RDFs are averages over all the ions as well as over the time span of the simulation. Hence, the fractional occupation number (0.4) of the first coordination sphere does mean that any one Mg(II) ion in the simulation has on average 0.4 phosphinyl oxygens in its first coordination sphere, which would imply exchange was observed. Indeed, no exchange of phosphinyl oxygens in the first coordination sphere was observed for any magnesium ion, which is evident from the RDF, which goes smoothly to zero after the first peak. Hence, each Mg(II) ion has an integer number of phosphinyl oxygens in its first coordination sphere (observed to be 1 or 0); the average over all ions is 0.4. The second coordination sphere is observed in the region 3.0–4.5 Å and is centered around 4.2 Å. The CN for this shell is 1.9. The interesting observation here is that Mg(II), on average, has $0.4 + 1.9 = 2.3$ phosphinyl oxygens in its first or second solvation shell. This comes about because some magnesium ions coordinate more than one (adjacent) phosphate at solvent separation during the simulation.

The RDF for Ca(II) has a sharp first coordination peak with similar magnitude to that of Mg(II), although somewhat broader. The peak is centered around 2.3 Å, with an average distance of 2.30 Å, very close to the value of 2.28 Å obtained from ab initio calculations of a Ca(II) ion bound to dimethylphosphate [25]. Again, the first and second coordination shells are well separated. The most noticeable difference in the RDF of the divalent ions is that the first CN for Ca(II), 0.9, is significantly greater than that of Mg(II) (0.4). This suggests that the population of phosphinyl oxygens in the first coordination sphere of Ca(II) is, on average, roughly twice that of Mg(II). On the other hand, the second CN for Ca(II) is 1.5, less than the 1.9 observed for Mg(II).

The RDF for Na(I) has the broadest first coordination peak centered around 2.2 Å, with an average first coordination distance and number of 2.24 Å, and 1.0, respectively. The first and second coordination shells in the RDF are less resolved than with the divalent ions, as seen in for $g_{ab}(r)$ and $n_{ab}(r)$ in the region 2.7–3.4

Na(I),Ca(II),Mg(II)--OA/OB

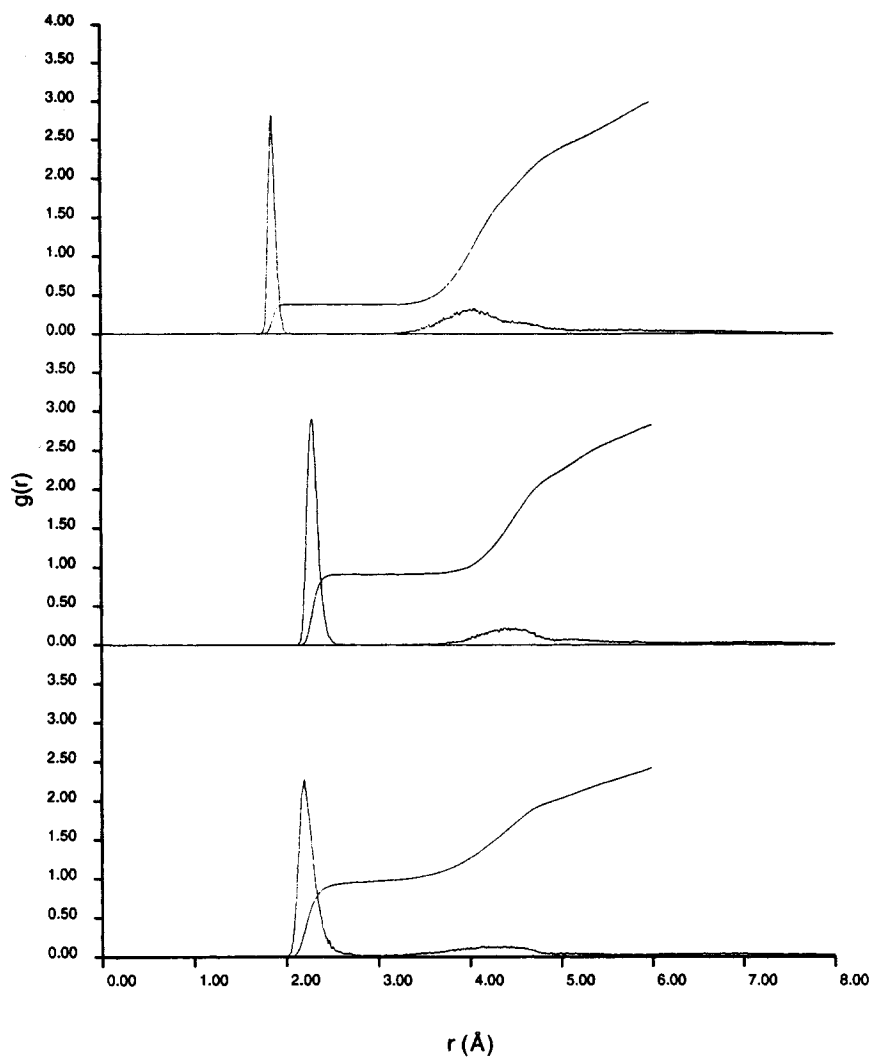


Figure 3. RDF and running CN for ions surrounded by phosphinyl oxygens.

TABLE III. Average coordination numbers (CN) and solvation distances ($\langle r \rangle$) of phosphinyl oxygens surrounding the various ions.

| Ion | MD | | | | EXP |
|---------|---------------------------|---------------------------|-----|-----|---------------------------|
| | $\langle r_1 \rangle$ (Å) | $\langle r_2 \rangle$ (Å) | CN1 | CN2 | $\langle r_1 \rangle$ (Å) |
| Na (I) | 2.24 ± 0.08 | 4.44 ± 0.28 | 1.0 | 1.0 | |
| Ca (II) | 2.30 ± 0.05 | 4.56 ± 0.26 | 0.9 | 1.5 | 2.28 |
| Mg (II) | 1.86 ± 0.03 | 4.23 ± 0.29 | 0.4 | 1.9 | 1.89 |

Comparisons of distances obtained from the simulations (MD) of the divalent ions are made with ab initio calculations (EXP) of divalent ions with dimethylphosphate [25].

Å; however, they are well defined. The second coordination peak centered around 4.4 Å is broader than for the divalent ions and has a CN of 1.0. Hence, on average, one phosphinyl oxygen is bound directly to a sodium ion (in its first coordination sphere) and one is bound at "solvent separation" (in its second coordination sphere).

The exchange rates of the phosphinyl oxygens were considerably slower than for water oxygens. No exchange of phosphinyl oxygens was observed in the first coordination sphere of the divalent ions during the 40 ps of MD. Exchange was observed in the first coordination sphere of the monovalent sodium ions, with an approximate lifetime of 15 ps. Exchange of phosphinyl oxygens in the second coordination sphere, however, was observed for all the ions. The exchange lifetimes were all on the order of 2 ps. These results are consistent with ab initio studies of Na(I) and Mg(II) metal ion interactions with a phosphate anion in the presence of two water molecules [35] that predict water can effectively compete with Na(I) for phosphate binding, but not with Mg(II).

B. Metal Ion-Phosphoester Oxygen (O3', O5') Interactions

Figure 4 shows the RDF of the phosphoester oxygens (O3', O5') around the metal ions. Table IV shows the corresponding average coordination numbers and distances. It is immediately evident from Figure 4 that none of the ions have phosphoester oxygens populating their first coordination spheres. The second coordination spheres are all asymmetric, with successively broader peaks in the order Mg(II) < Ca(II) < Na(I). The observed broadening of the peaks reflects the overall degree of delocalization of the ions around the phosphate anions.

4. Discussion

To probe the interaction of the metal ions with the phosphinyl oxygens more closely, we considered the distribution of metal ions around the phosphate anions. RDFs of the ions around the phosphinyl oxygens are not shown, since they provide essentially the same information as do the RDFs of the phosphinyl oxygens around the ions.

Figures 5, 6, and 7 show scatter plots (from three orthogonal views) of the ionic distributions around the phosphate anions between 10 and 40 ps of the MD sim-

Na(I),Ca(II),Mg(II)--O3'/O5'

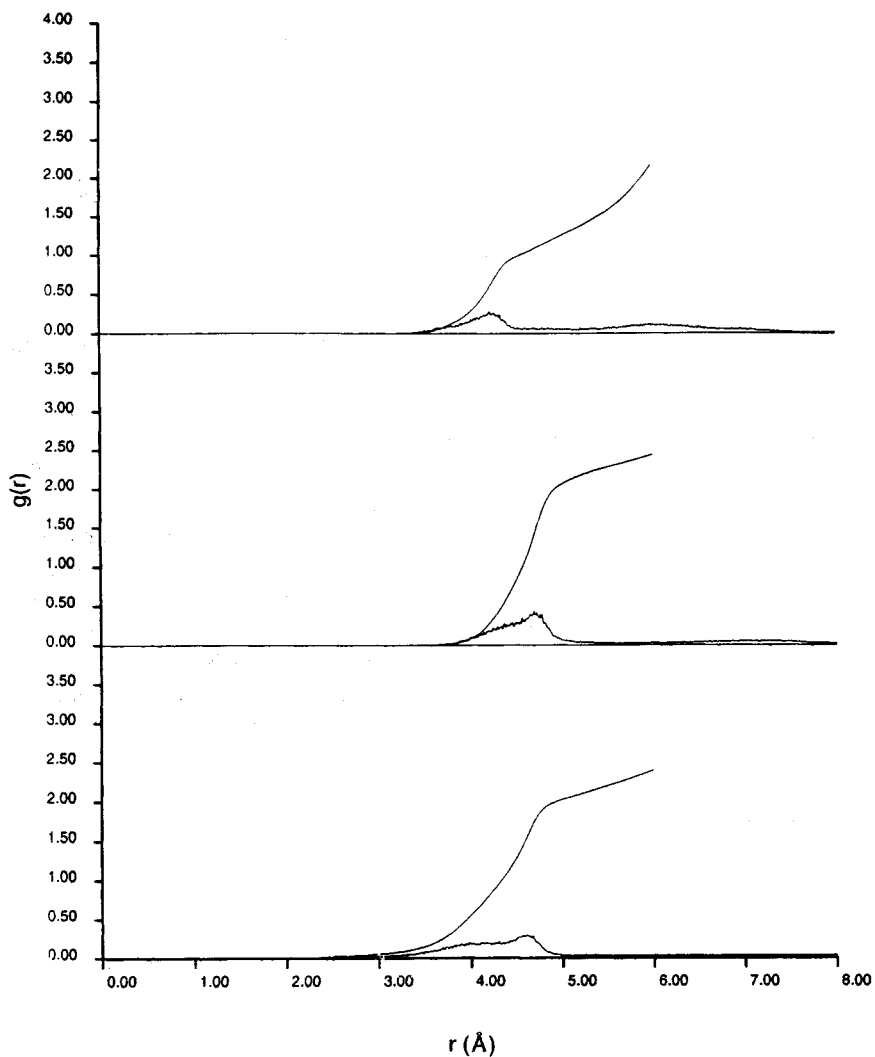


Figure 4. RDF and running CN for ions surrounded by phosphoester oxygens (O3'/O5').

TABLE IV. Average coordination numbers (CN) and solvation distances ($\langle r \rangle$) of phosphoester oxygens surrounding the various ions.

| Ion | $\langle r_1 \rangle$ (Å) | $\langle r_2 \rangle$ (Å) | CN1 | CN2 |
|---------|---------------------------|---------------------------|-----|-----|
| Na (I) | — | 4.47 ± 0.26 | — | 1.8 |
| Ca (II) | — | 4.62 ± 0.22 | — | 2.2 |
| Mg (II) | — | 4.44 ± 0.12 | — | 1.2 |

ulation for Na(I), Ca(II), and Mg(II), respectively. From the figures, it can be seen that Mg(II) is highly localized when coordinated directly to the phosphate oxygen and that Mg(II) prefers a unidentate orientation. Additionally, Mg(II) displays a significant population in an ordered second coordination sphere around the phosphate anions. The Ca(II) ions also prefer a unidentate orientation to the phosphinyl oxygens; however, Ca(II) ions are less localized than the Mg(II) ions when directly coordinated to the phosphate anions. Unlike the Mg(II) ions, the Ca(II) ions do not have a significant population in the second coordination sphere around the phosphate anions. The Na(I) ions are significantly more delocalized around the phosphate anions than are the divalent ions. The Na(I) ions appear to prefer a unidentate orientation; however, unlike the divalent ions, a small contribution of direct bidentate coordination is also observed with sodium. It is evident from these figures that the various ions are distributed quite differently around the phosphate anions of the DNA.

The orientation of the ions coordinated to the phosphate oxygens can be described as either *syn* or *anti*, analogous to the description of metal ion–carboxylate orientation [36] (Fig. 8). Additionally, other parameters are useful in describing metal ion binding to phosphate anions such as the P=O—Me angle and the distance of the metal from the plane of the phosphate. Table V shows the average P=O—Me angle, average distance of the metal ions from the plane of the phosphate, and the percent occupation of *syn* and *anti* orientation of the directly coordinated ions. These results are compared to a recently published statistical analysis of phosphinyl–metal ion structures obtained from the Cambridge Structural Database [37]. The results from the MD simulations are clearly in qualitative agreement with the statistical results. The Ca(II) ion has the largest P=O—Me angle and *syn/anti* orientation ratio and the smallest out-of-plane distance. However, within the margin of error, each of the ions is qualitatively similar in each of these parameters.

Figure 9 shows a histogram of the distribution of first CNs (all oxygens) for each ion. Na(I) shows the broadest distribution in CNs, having a maximum probability of 5 (59.7%). Ca(II) has a more narrow distribution with maximum probability of 8 (63.8%), however, with significant probability of CN 7 (34.3%). Mg(II) has a very stable first coordination sphere with CN 6.0, which is the only significantly observed state.

An interesting question concerning the binding of a hydrated metal ion to a polyelectrolyte is how is the hydration number changes upon binding, i.e.; How



Figure 5. Scatter plots of the distribution of Na(1) ions around the phosphates. Three orthogonal projections are shown: (1) plane of the phosphate anion (containing O—P—O atoms); (2) plane bisecting the phosphinyl oxygens; and (3) plane perpendicular to (1) and (2). The phosphinyl oxygens are in the horizontal direction; the phosphoester oxygens are in the vertical direction.

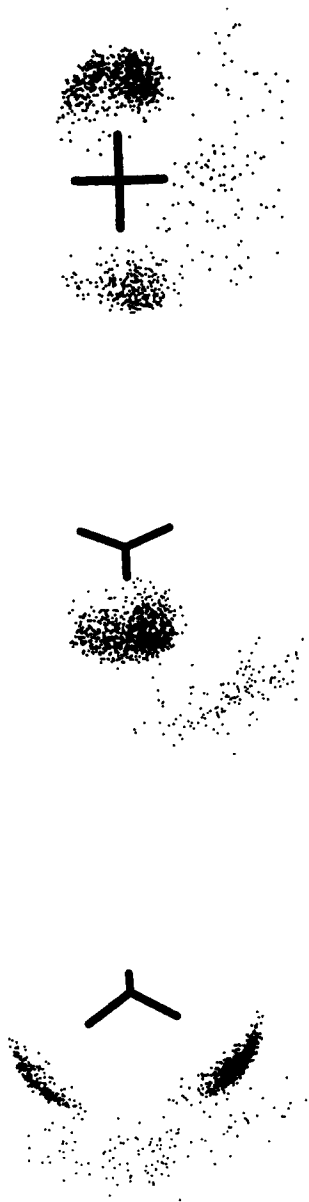


Figure 6. Scatter plots of the distribution of Ca(II) ions around the phosphates. Three orthogonal projections are shown: (1) plane of the phosphate anion (containing $\text{O}-\text{P}-\text{O}$ atoms); (2) plane bisecting the phosphinyl oxygens; and (3) plane perpendicular to (1) and (2). The phosphinyl oxygens are in the horizontal direction; the phosphoester oxygens are in the vertical direction.

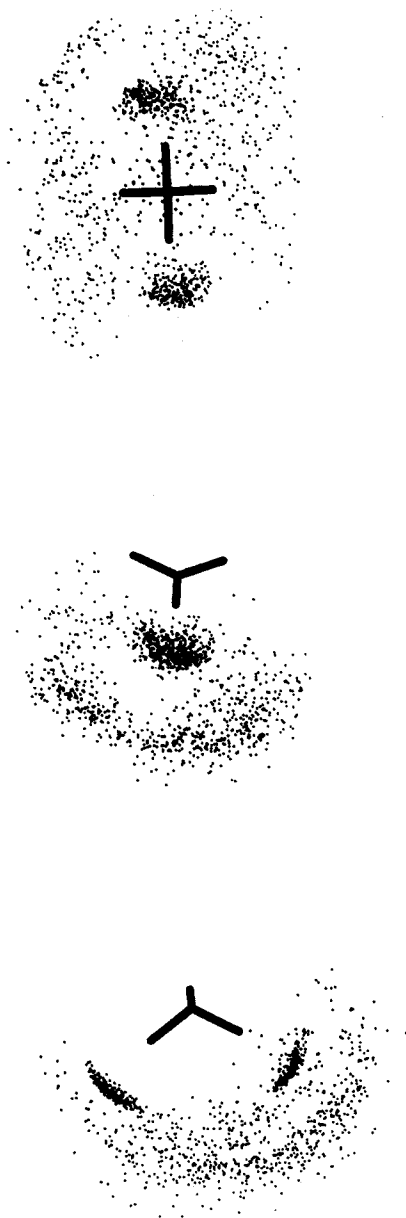


Figure 7. Scatter plots of the distribution of Mg(II) ions around the phosphates. Three orthogonal projections are shown: (1) plane of the phosphate anion (containing O—P—O atoms); (2) plane bisecting the phosphinyl oxygens; and (3) plane perpendicular to (1) and (2). The phosphinyl oxygens are in the horizontal direction; the phosphoester oxygens are in the vertical direction.

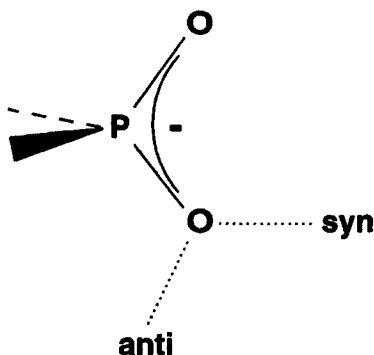


Figure 8. Schematic drawing of metal ion coordinated to a phosphate anion showing the *syn* and *anti* ligand orientations.

many water molecules hydrate the ion prior its binding and how many remain after it is bound? To answer this question, statistics were obtained separately from the simulations for metal ions bound directly to the phosphate anions (i.e., while the ions contained a phosphinyl oxygen in their first coordination sphere) and for metal ions that had a first coordination sphere entirely occupied by water but still associated to the phosphate anions at solvent separation. Figures 10 and 11 show histograms of the hydration numbers (of water oxygens) for ions unbound and bound to the phosphate anions, respectively. Na(I) ions not directly coordinated to the phosphate exhibit a broad distribution of CNs having similar probabilities of 5 (50.8%) and 6 (42.1%). Upon direct coordination to the phosphinyl oxygen, the water oxygen hydration number stabilizes somewhat, having a maximum probability at 4 (62.0%) and, hence, an overall CN of 5 [4 water oxygens + 1 phosphinyl oxygen]. The first hydration sphere for an unbound Ca(II) ion becomes broader with ligand binding. The most probable hydration state for the unbound ion is 8 (84.2%). Upon direct coordination of a phosphinyl oxygen, the most probable

TABLE V. Metal ion orientation parameters: P=O—Me angle, distance of the metal ion from the plane of the phosphate anion (distance), and percent *syn* and *anti* orientation.

| Ion | P=O—Me (deg) | Distance ^a (Å) | % <i>syn</i> | % <i>anti</i> |
|---------|-----------------|------------------------------|--------------|---------------|
| Na (I) | 135.4 ± 18.7 | 0.98 ± 0.32 | 63 | 37 |
| Ca (II) | 149.1 ± 17.3 | 0.72 ± 0.33 | 82 | 18 |
| Mg (II) | 137.7 ± 22.3 | 0.92 ± 0.40 | 78 | 22 |
| EXP | 141 ± 14 | 0.9 ± 0.5 | 63 | 37 |

Comparisons of the results obtained from the simulations are made with statistical analysis of metal ion–phosphate structures in the Cambridge Structural Database (EXP) [37].

^a Average distance from the plane of the phosphate.

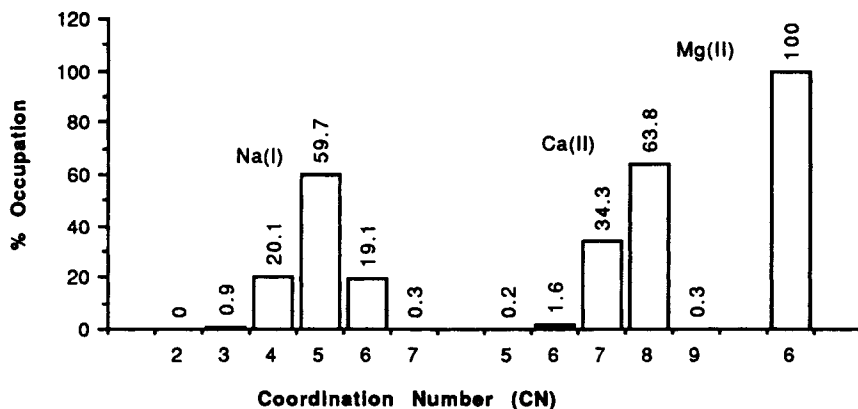


Figure 9. Histograms of the CN for each ion showing the percent occupation of each coordination state. Coordination to any oxygen (water, phosphinyl, or phosphoester) is shown.

water oxygen hydration number becomes 7 (61.8%) with significant probability of 6 (35.7%) as well. The average water oxygen CN of the unbound calcium ion (7.9) reduces to 6.6 upon direct coordination of the phosphinyl oxygen. Hence, the first coordination sphere of Ca(II) appears to be less structured upon ligand binding, and the average CN is lowered slightly. Mg(II) ions are observed to require a CN of 6.0 regardless of whether it is directly bound to the phosphate anions or not.

NMR studies [38–40] have revealed that divalent metal ions exhibit two distinct types of binding to DNA. Cations that are not directly bound to any one site of the DNA, but instead are delocalized around the polymer due to its net negative charge, and, hence, easily displaced by titration of different ions at high concentra-

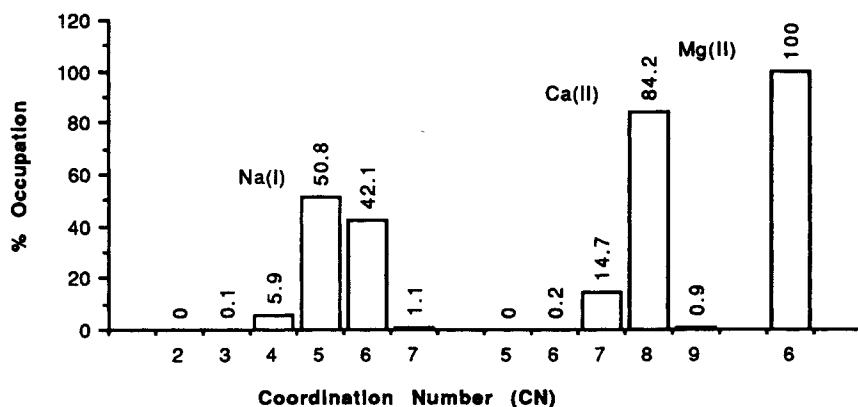


Figure 10. Histograms of the hydration number (of water oxygens only) for unbound ions (ions not directly coordinated to the phosphate anions) showing the percent occupation of each hydration state.

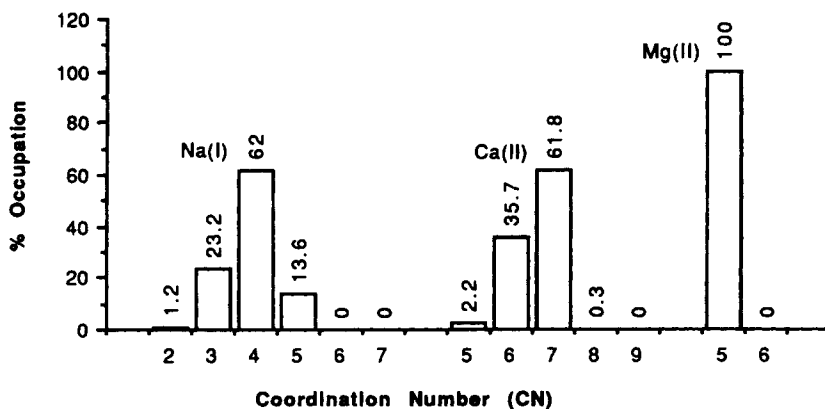


Figure 11. Histograms of the hydration number (of water oxygens only) for bound ions (ions directly coordinated with a phosphinyl oxygen) showing the percent occupation of each hydration state.

tions, are said to be “territorially-bound” [38]. Ions that are directly bound to particular sites of the DNA, and are not easily displaced by other competing ions, are said to be “site-bound.”

The description of territorially bound ions can to a large extent be described adequately by modeling the DNA as a infinite cylinder of negative charge and treating the ionic distribution around the cylinder by solving the Poisson–Boltzmann (PB) equation [7]. This technique has been used to predict the distribution and electric fields of monovalent and divalent ions around DNA [41]. Additionally, the ion condensation model proposed by Manning [8] also provides a reasonable description of territorially bound ions. These descriptions, however, do not predict the behavior of site-bound ions in which the hydration state plays a decisive role. An alternative procedure for examining site-bound ions is to perform large computer modeling simulations treating ions explicitly as we have done here. Recent NMR studies have shown that divalent magnesium [38,39] and calcium [40,42] ions show both territorial-binding and site-binding character. Monovalent sodium ions, however, show predominantly territorial-binding character [13,40]. Results of our MD study support these notions, since Na(I) ions seem to be much more delocalized around the phosphate anions and exhibit more rapid exchange when directly coordinated to the phosphinyl oxygens.

It has been suggested in the literature that magnesium ions have a higher affinity for site binding than for calcium [40], since titration with calcium is unable to remove all of the site-bound magnesium ions, whereas the reverse titration with magnesium can displace all the calcium. Furthermore, it has been shown by CD [43] and UV [44] experiments that alkaline earth metals interact predominantly with the phosphate residues of the DNA. Recent Raman spectroscopic studies have suggested comparable amounts of Ca(II) and Mg(II) are bound to the phosphate anions [20]. The measure used in this study for determination of site binding of

divalent metal ions to the phosphate anions was a decrease in intensity of the 1093 cm^{-1} band, arising from the symmetric PO_2^- stretch, which would be affected by covalent interactions of the metal ions directly with the phosphinyl oxygens. Electrostatic interactions with hydrated ions, however, are not believed to modify this band appreciably. Furthermore, NMR experiments have predicted that the exchange rate for Mg(II) with the phosphate anions is faster than for Ca(II) [42]. A plausible reason suggested by our studies for this behavior is reflected in the hydration states of the bound ions. The Mg(II) ions, having a very stable first hydration sphere, are able to remain localized around the phosphate anions while maintaining a full hydration sphere of water and, thus, are bound to a particular site as a hydrated cation. Since the exchange rate of water in the first hydration sphere of magnesium is much slower than that for calcium, on the order of 10^6 times longer [36], one would expect that water could more effectively compete with the phosphinyl oxygens for direct coordination with magnesium than for calcium. Ca(II) ions, on the other hand, exchange water molecules much more quickly, and thus provide more frequent opportunity for a phosphinyl oxygen to enter its coordination sphere.

5. Conclusion

The results of our MD investigation of ion binding to DNA suggest that sodium ions are highly delocalized around the phosphate residues and, on average, directly coordinate one of the phosphinyl oxygens. Na(I) prefers to have 5 oxygen moieties in its first coordination sphere; however, significant populations of 4 and 6 coordinate geometries are also observed. Upon direct coordination of a phosphinyl oxygen ligand, an increase in hexacoordination is observed (from 19.1% to 42.1%). Furthermore, exchange of both waters and phosphinyl oxygens was observed in the first solvation sphere of sodium on the time scale of the simulation (40 ps). Divalent calcium ions were more localized around the phosphate anions, with mostly unidentate orientation and direct coordination to the phosphinyl oxygens. Unbound calcium ions predominantly have 8 water oxygens in the first coordination sphere. Directly coordinated calcium ions generally have 7 water oxygens in its first coordination sphere in addition to the phosphinyl oxygen ligand; however, a significant population of calcium ions have only 6 water oxygens. Hence, a decrease was observed in the population of 8 coordinate ions (84.2% to 61.8%) with a corresponding increase in population of 7 coordinate ions (14.7% to 35.7%). Exchange of waters in the first hydration sphere of calcium was observed during the simulation, with an average lifetime of 2 ps; however exchange of phosphinyl oxygens was not observed. Magnesium ions were observed to be both highly localized around the phosphate anions when bound directly and delocalized around the phosphate anions as a fully hydrated ion. Magnesium ions were observed to be strictly hexacoordinated throughout the simulation, and no exchange of water oxygens or phosphinyl oxygens was observed. Directly bound magnesium ions were observed exclusively in the unidentate orientation; however, the majority of the magnesium ions, unlike calcium, were not directly bound to the phosphate anions, but interacted at solvent separation as hydrated ions. None of the ions in this study was observed to interact

directly with the phosphoester oxygens and only mildly in the second solvation shell, probably as a result of association with the nearby phosphinyl oxygens.

The simulations described herein show encouraging agreement with experimental results and ab initio calculations and demonstrate the usefulness of molecular dynamics as a technique for investigating ion–polyelectrolyte interactions in an explicit manner.

Acknowledgments

D.Y. thanks the Pittsburgh and North Carolina Supercomputing Centers for computer time and use of their facilities. L.G.P. acknowledges NIH for support through Grant HL-27995 and NIEHS for use of their facilities through an EXPERT appointment.

Bibliography

- [1] C. L. Eichhorn, *Nature* **194**, 474 (1962).
- [2] C. L. Eichhorn and Y. A. Shin, *J. Am. Chem. Soc.* **90**, 7323 (1968).
- [3] R. W. Wilson and V. A. Bloomfield, *Biochemistry* **18**, 2192 (1979).
- [4] C. L. Eichhorn, Y. A. Shin, and J. J. Butzow, *Cold Spring Harbor Symp. Quant. Biol.* **47**, 125 (1983).
- [5] S. Silverand and T. K. Misra, *Annu. Rev. Microbiol.* **42**, 717 (1988).
- [6] T. D. Tullius, Ed., *Metal-DNA Chemistry* (American Chemical Society, Washington, DC, 1989).
- [7] A. Katchalsky, *Pure Appl. Chem.* **26**, 327 (1971).
- [8] G. S. Manning, *Q. Rev. Biophys.* **11**, 179 (1978).
- [9] G. Pack, G. Lamm, L. Wong, and D. Clifton, in *Theoretical Biochemistry & Biophysics* (Adenine Press, New York, 1990).
- [10] G. Pack, L. Wong, and G. Lamm, *Int. J. Quantum Chem., Quantum Biol. Symp.* **16**, 1 (1989).
- [11] C. F. Anderson, M. T. Record, Jr., and P. A. Hart, *Biophys. Chem.* **7**, 301 (1978).
- [12] M. L. Bleam, C. F. Anderson, and M. T. Record, Jr., *Biopolymers* **22**, 5418 (1983).
- [13] W. H. Braunlin, C. F. Anderson, and M. T. Record, Jr., *Biopolymers* **25**, 205 (1986).
- [14] K. N. Swamy and E. Clementi, *Biopolymers* **26**, 1901 (1982).
- [15] G. L. Seibel, U. C. Singh, and P. A. Kollman, *Proc. Natl. Acad. Sci. U.S.A.* **82**, 6537 (1985).
- [16] W. F. Van Gunsteren and H. J. C. Berendsen, in *Proceedings of the Workshop on Molecular Dynamics and Protein Structure*, J. Hermans, Ed. (Polycrystal Book Service, Western Springs, IL, 1985).
- [17] S. Swaminathan, G. Ravishanker, and D. Beveridge, *J. Am. Chem. Soc.* **113**, 5027 (1991).
- [18] E. Clementi and R. H. Sarma, Eds., *Structure and Dynamics: Nucleic Acids and Proteins* (Adenine Press, New York, 1986) pp. 321–362.
- [19] B. Jayaram and D. L. Beveridge, *J. Phys. Chem.* **95**, 2506 (1991).
- [20] M. Langlais, H. A. Tajmir-Riahi, and R. Savoie, *Biopolymers* **30**, 743 (1990).
- [21] R. Wing, H. Drew, T. Takano, C. Broka, S. Tanaka, K. Itakura, and R. E. Dickerson, *Nature* **287**, 755 (1980).
- [22] S. J. Weiner, P. A. Kollman, D. A. Case, U. C. Singh, C. Chio, G. Alagona, S. Profeta, and P. Weiner, *J. Am. Chem. Soc.* **106**, 765 (1984).
- [23] P. K. Weiner and P. A. Kollman, *J. Comp. Chem.* **2**, 287 (1981).
- [24] S. J. Weiner and P. A. Kollman, *J. Comp. Chem.* **7**, 230 (1986).
- [25] D. W. Deerfield, H. B. Nicholas, Jr., R. G. Hiskey, and L. G. Pedersen, *Proteins* **6**, 168 (1989).
- [26] D. W. Deerfield II, M. A. Lapadat, L. L. Spremulli, R. G. Hiskey, and L. G. Pedersen, *J. Biomol. Struct. Dyn.* **6**, 1077 (1989).
- [27] W. L. Jorgensen, *J. Am. Chem. Soc.* **103**, 335 (1981).

- [28] M. P. Allen and D. J. Tildesley, Eds., *Computer Simulations of Liquids* (Clarendon Press, Oxford, 1987).
- [29] G. Palinkas, W. O. Riede, and K. Heinzinger, *Z. Naturforsch.* **A32**, 1137 (1977).
- [30] M. M. Probst, T. Radnai, and K. Heinzinger, *J. Phys. Chem.* **89**, 753 (1985).
- [31] N. A. Hewish, G. W. Neilson, and J. E. Enderby, *Nature* **297**, 138 (1982).
- [32] G. Palinkas, W. O. Riede, and K. Heinzinger, *Z. Naturforsch.* **A37**, 1049 (1982).
- [33] P. A. Kollman and I. D. Kuntz, *J. Am. Chem. Soc.* **94**, 9236 (1973).
- [34] H. L. Friedman, *Chem. Scr.* **25**, 42 (1985).
- [35] C. V. Prasad and G. R. Pack, *J. Am. Chem. Soc.* **106**, 8079 (1984).
- [36] C. J. Carrell, H. L. Carrel, J. Erlebacker, and J. P. Glusker, *J. Am. Chem. Soc.* **110**, 8651 (1988).
- [37] R. S. Alexander, Z. F. Kanyo, L. E. Chirlian, and D. W. Christianson, *J. Am. Chem. Soc.* **112**, 933 (1990).
- [38] D. M. Rose, M. L. Bleam, M. T. Record, Jr., and R. G. Bryant, *Proc. Natl. Acad. Sci. U.S.A.* **77**, 6289 (1980).
- [39] D. M. Rose, C. F. Polnaszek, and R. G. Bryant, *Biopolymers* **21**, 653 (1982).
- [40] W. H. Braunlin, T. Drakenberg, and L. Nordenskiold, *Biopolymers* **28**, 1339 (1989).
- [41] G. Pack, *Int. J. Quantum Chem., Quantum Biol. Symp.* **10**, 61 (1983).
- [42] P. Reimarsson, J. Parello, T. Drakenberg, H. Gustavsson, and B. Lindman, *FEBS Lett.* **108**, 439 (1979).
- [43] C. Zimmer, G. Luck, and H. Triebel, *Biopolymers* **13**, 425 (1974).
- [44] R. G. Bhattacharyy, K. K. Nayak, and A. N. Chakrabarty, *Inorg. Chim. Acta* **153**, 79 (1988).

Received March 14, 1992

Revised manuscript received May 12, 1992

Accepted for publication May 13, 1992